Biochemical and Biophysical Research Communications 450 (2014) 1668–1672

Contents lists available at ScienceDirect

Biochemical and Biophysical Research Communications

journal homepage: www.elsevier.com/locate/ybbrc

The kinetics of thermal stress induced denaturation of Aquaporin 0

John E. Hansen [a,*], Logan Leslie [a], Satyanarayana Swamy-Mruthinti [b]

[a] Department of Chemistry, University of West Georgia, Carrollton, GA 30118, USA
[b] Department of Biology, University of West Georgia, Carrollton, GA 30118, USA

ARTICLE INFO

Article history:
Received 1 July 2014
Available online 17 July 2014

Keywords:
Aquaporin 0
Denaturation
Aggregation
Secondary structure
Circular Dichroism
α-Crystallin

ABSTRACT

Aquaporin 0 (AQP0) is an integral membrane protein that facilitates water transport and cellular adhesion in the lens. Its dysfunction has been associated with cataractogenesis. Our earlier studies showed AQP0 undergoes aggregation when subjected to thermal stress and this aggregation seems to have been facilitated by mechanical agitation brought about by gentle stirring. The purpose of this study is to determine the secondary structural changes that precede aggregation and the role that α-crystallin plays in inhibiting those structural changes. Detergent solubilized calf lens AQP0 was subjected to thermal stress at 50 °C for varying times. Secondary structural changes were measured by Circular Dichroism (CD) spectropolarimetry. Convex constraint analysis was used to deconvolute the CD spectra into pure component curves representing the secondary structural elements. Our results showed that under thermal stress, the α-helix content of AQP0 decreased from 50% to 7% with a concomitant increase from 0% to 52% in β-sheet content. The time-dependent loss of α-helical structure and gain of β-sheet structure appear to follow first-order kinetics with very similar values (~30 min) suggesting a single transition. In the presence of α-crystallin, this conversion to β-sheet is minimized, suggesting that the protein structure that binds to the molecular chaperone is mostly the α-helical structure of AQP0.

© 2014 Elsevier Inc. All rights reserved.

1. Introduction

Conformational transitions in proteins that lead to aggregation have drawn significant attention over the last couple decades, since they have been recognized in the etiology of a number of diseases. Recent studies have focused on the early steps in aggregate formation, beginning with a conformational change in protein structure that triggers oligomeric formation [1]. Due to the fact that characterizing these transitions are experimentally challenging, molecular dynamic simulations have been used to provide a theoretical understanding [2], nonetheless, the nature of these transitions remain largely unresolved.

Until relatively recently it had been thought that protein aggregation was a nonspecific reaction initiated by non-native contacts between proteins in partially unfolded states [3], however, over the last decade an increasing number of studies suggest that the process can be correlated to certain physiochemical parameters [4,5]. Several models for aggregation do point to changes in protein secondary structures that initiate the formation of an intramolecular β-sheet. Often the initial step is a large conformational rearrangement involving the α-helical to β-sheet transition [6].

A number of factors have been identified that effect aggregation of a protein in the native state, including oxidative stresses, changes in pH, chemical denaturants, and thermal stress [7]. Living organisms respond, at the cellular level, to stressful conditions by increased expression of heat shock proteins (HSPs), which function as molecular chaperones. Under stressful conditions they interact with partially unfolded non-native structures of the target protein, thus preventing misfolding and aggregation. Following the period of stress, molecular chaperones will assist in protein refolding, salvage and degradation of unrecoverable proteins [8]. Of particular interest to our study is α-crystallin, belonging to the family of small heat shock proteins (HspB4 and HspB5), which was shown to exhibit molecular chaperone-like activity in preventing the thermal stress induced aggregation of other proteins [9,10].

Transmembrane proteins transport solutes and ions across cell membranes, thus play a crucial role in cellular homeostasis. Loss of structural integrity of these transmembrane proteins, brought about by metabolic or environmental stresses, may lead to altered function. Aquaporins are a family of transmembrane proteins comprised of six-helix bundles, which are arranged as tetramers within cell membranes; each monomer functioning as a water channel

Abbreviations: AQP0, Aquaporin 0; OG, octyl-β-D glucopyranoside; CD, Circular Dichroism; CCA, Constant Constraint Algorithm; HT, High Tension.

* Corresponding author. Address: Department of Chemistry, 1601 Maple St., University of West Georgia, Carrollton, GA 30118, USA.
E-mail address: jhansen@westga.edu (J.E. Hansen).

http://dx.doi.org/10.1016/j.bbrc.2014.07.056
0006-291X/© 2014 Elsevier Inc. All rights reserved.

[11]. Aquaporin 0 (AQP0) is the first cloned member of the Aquaporin family of proteins [12], expressed exclusively in the lens fiber cells. As per the model proposed by Mathias and Rae [13], AQP0 channels play an important role in micro-circulation of nutrients and wastes in the lenses. Furthermore, AQP0 is also shown to have cell-to-cell adhesion function in the lens [14,15]. Recently we have shown that thermal stress, coupled with mechanical agitation, of the detergent-solubilized AQP0 induced aggregation, and this aggregation was significantly reduced in the presence of α-crystallin [16]. In order to understand a possible mechanism for the protein structural transition preceding aggregation, we followed the secondary structural changes of AQP0 during thermal stress. We also showed the role of α-crystallin in preventing these changes.

2. Materials and methods

2.1. Lenses

Calf lenses were purchased from Pelfreeze, (Little Rock, AK) and stored at −80 °C until use. Decapsulated calf lenses were homogenized in ice-cold PBS (Sigma chemicals, St. Louis, MO), and centrifuged at 18,000×*g* for 15 min at 4 °C. The soluble fraction was used to isolate α-crystallin as described elsewhere. The pellet was washed sequentially twice with PBS, twice with 7 M urea (prepared in PBS) and again twice with PBS. The pellet was recovered by centrifugation at 18,000×*g* for 15 min at 4 °C. The membrane pellet was resuspended in PBS and used in this assay.

2.2. Solubilization of AQP0

AQP0 was selectively solubilized in 2% non-ionic detergent octyl β-D-glucopyranoside (OG) from Calbiochem, La Jolla, CA). Solubilized AQP0 was recovered by centrifugation at 12,000 rpm for 12 min at 4 °C. Protein content was estimated by BCA protocol (Kit from Pierce, Rockford, IL), using bovine serum albumin in 2% OG as the standard.

2.3. Purification of α-crystallin

Bovine α-crystallin was purified from the calf lens soluble fraction by Sephacryl S-300 HR gel permeation chromatography [17].

2.4. CD spectral measurements

All Circular Dichroism (CD) spectra were measured on a Jasco 715 spectropolarimeter, equipped with a Peltier temperature controller. The instrument was purged with pre-purified nitrogen at a flow rate of 8 L/min. Spectra were measured between 190 and 260 nm with a band-width of 1.0 nm, scan rate of 20 nm/min and time constant of 2 s. A total of 8 scans were averaged. Buffer and detergent concentrations were optimized and set so that the High Tension (HT) voltage applied to the photomultiplier tube would be less than 700 volts at wavelengths longer than 190 nm.

The concentration of detergent-solubilized AQP0 was 0.2 mg/ml. In those experiments where chaperone function was studied, the bovine α-crystallin was added at a concentration of 0.2 mg/ml. The detergent concentration was maintained at 2% in all experiments. Samples were placed in a 0.05 cm detachable quartz cell. Temperature of samples was rapidly raised to 50 °C and held there for a specified time. The temperature was then rapidly lowered to 20 °C and held at that temperature for 5 min prior to recording the CD spectrum. Background spectra were collected in the same fashion for the buffer solution containing the detergent. For those samples that contained α-crystallin, the solutions that were used for their background spectra also contained α-crystallin at the same concentration. Corrected spectra (after subtracting the background spectra) were converted to molar ellipticity by $[\theta] = \theta M/(10lcn)$ (deg cm^2/dmol) using the measured ellipticity (θ, deg), molar mass (M, 28,511 g/mol), protein concentration (c, g/cm^3), cuvette path length (l, 0.05 cm), and number of amino acid residues (n, 269). In order to determine the degree of aggregation, HT voltage traces (between 185 and 260 nm) were recorded along with each CD spectrum.

Deconvolution of the CD spectra into pure component spectra was accomplished using the Constant Constraint Algorithm (CCA), which was included in the manufacturer's software package (Jasco Inc.). The time courses generated from plotting the fraction of secondary component against incubation time were fit to exponential functions. The fitting procedure employed the Levenberg–Marquardt algorithm (Origin version 7.5).

3. Results

The goal of this study is to analyze the secondary structural changes that precede aggregation of AQP0. The left panel of Fig. 1 displays the CD spectra of detergent solubilized AQP0 held at 50 °C for different incubation times, particularly noticeable is the decrease in ellipticity for the band at 209 nm with increasing incubation time. It is also worth noting that there is a well-defined isosbestic point near 200 nm for the overlaid spectra (Fig. 1, left panel).

In the presence of α-crystallin, the thermally induced structural changes of AQP0 were greatly reduced (see right panel of Fig. 1). The decrease in ellipticity at 209 nm was significantly less for the spectra collected over the same incubation time than when α-crystallin is absent. Furthermore, unlike the AQP0 spectra (displayed in the left panel), the overlaid spectra of the AQP0 + α-crystallin (displayed in the right panel) do not exhibit a well-defined isosbestic point (Fig. 1).

The specific structural changes that occur during the thermal denaturation of AQP0 can be elucidated by deconvoluting the CD spectra into characteristic CD signatures. The CCA was employed to deconvolute the CD spectra into the "pure"-component curves displayed in Fig. 2. Using the priori method described by Fasman's group [18], it was determined that a minimum number of four pure curves were necessary to adequately reconstruct all the measured CD spectra. Each pure curve exhibits the signatures of a specific secondary structural element. The pure curve represented by the solid line shows α-helical character, with two bands of negative ellipticity located at 210 and 225 nm and the dashed line is indicative of β-sheet structure, and the remaining two curves are typical spectral features of unordered structures (Fig. 2, left panel) [18,19].

Each measured CD spectrum in Fig. 1 can be reconstructed from a unique linear combination of the four pure component curves. Right panel in Fig. 2 compares measured spectra from Fig. 1 with reconstructed spectra, $f(\lambda)$, as defined by $f(\lambda) = C_{\alpha\text{-helix}} \times g_{\alpha\text{-helix}}(\lambda) + C_{\beta\text{-sheet}} \times g_{\beta\text{-sheet}}(\lambda) + C_{\text{random-I}} \times g_{\text{random-I}}(\lambda) + C_{\text{random-II}} \times g_{\text{random-II}}(\lambda)$. The functions, $g_i(\lambda)$, are the individual pure component curves shown in Fig. 2 (left panel). The weighted coefficients, C_i, are the secondary structural percentages of a protein determined by the CCA program. The sum of the weighted coefficients of each protein must equal unity,

$$\sum_{i=1}^{4} C_i = 1$$

In Fig. 3, the fractions of α-helix and β-sheet components are plotted against the incubation time. The plots displayed in the left panel reveal decreasing α-helix content and concomitant increasing β-sheet content during the thermal denaturation of detergent solubilized AQP0. The time courses for the change in α-helix content and β-sheet content were fit to the following exponential function:

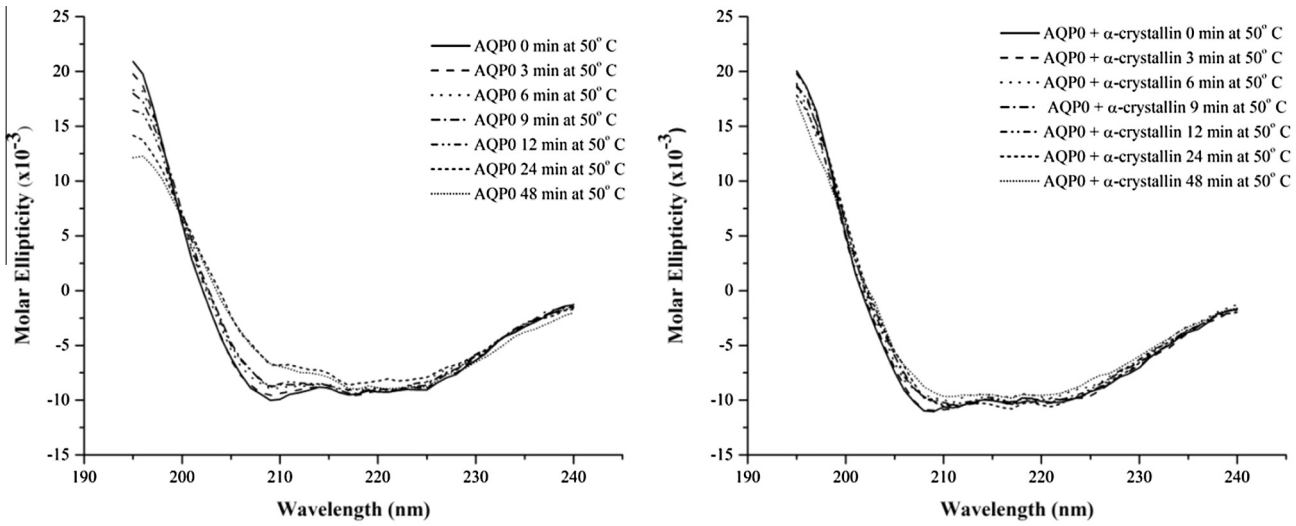

Fig. 1. CD spectra of detergent-solubilized AQP0 under thermal stress. AQP0 (0.2 mg/ml in 2% octyl glucoside in PBS) was heated to 50 °C for different incubation times. Left panel displays spectra of AQP0 without α-crystallin. The right panel displays spectra of AQP0 in the presence of α-crystallin (0.2 mg/ml). Spectra were collected after the temperature of the solution was rapidly lowered to 20 °C, following incubation at 50 °C for 0 min (—), 3 min (– –), 6 min (• • •), 9 min (– • –), 12 min (– • • –), 24 min (- - -), and 48 min (····). Note a well-defined isosbestic point near 200 nm in the left panel and absence thereof in the right panel.

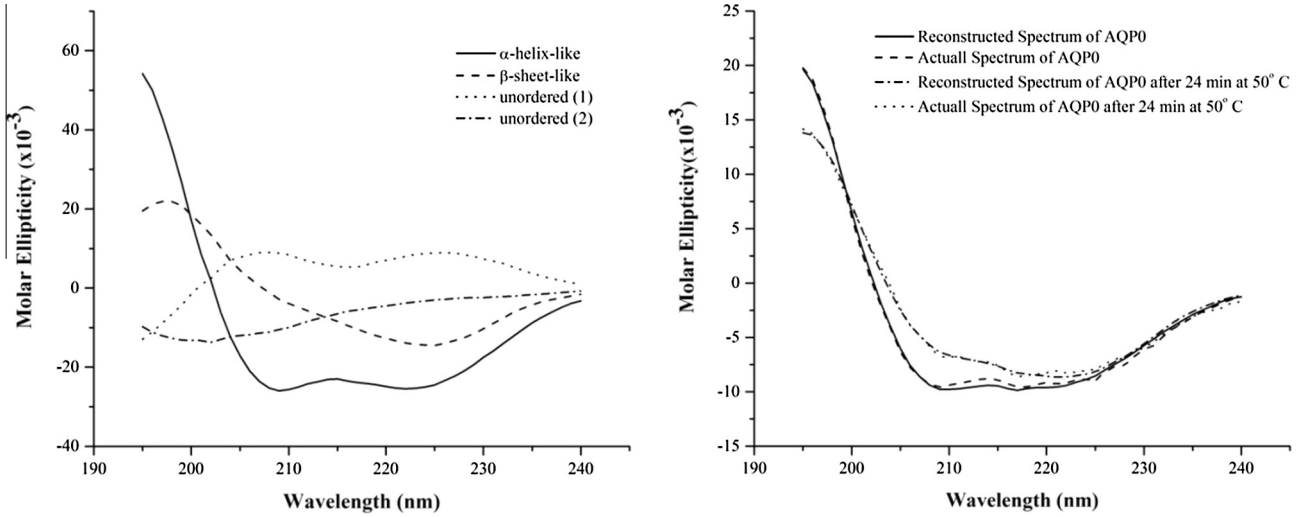

Fig. 2. Deconvolution of CD spectra of AQP0 into pure components. Left panel: These are the pure component curves generated by applying the convex constraint algorithm to deconvolute the CD spectra recorded for AQP0 under thermal stress. The four pure curves displayed represent a α-helix-like component (—), a β-sheet-like component (– –), an unordered component I (• • •), and an unordered component II (– • –). Right panel: The CD spectrum (—) reconstructed from the pure components is compared with the measured CD spectrum (– –) for AQP0 not subjected to thermal stress. The reconstructed CD spectrum (– • –) is compared with the measured CD spectrum (• • •) for AQP0 subjected to thermal stress at 50 °C for 24 min.

$$y(t) = y_0 + A\exp(-t/T)$$

where t is the incubation time and y is the fraction of pure component. The parameters y_0, A and T are listed in Table 1. The time constant, T, for the exponential decay in α-helix content was found to be nearly identical to the time constant for the exponential rise in β-sheet content (about 30 min).

The right panel of Fig. 3 displays a plot for the fraction of α-helix and β-sheet components when α-crystallin is present during the thermal denaturation. The time courses representing the decrease in α-helical content and the increase in β-sheet content were also fit to the above exponential function. As shown in Table 1, the pre-exponential amplitudes (A) are significantly smaller for these time courses than those shown in the left panel compared to right panel of Fig. 3, indicating that changes in secondary structure are considerably reduced when α-crystallin is present.

Fig. 4 shows the HT voltage traces associated with the CD spectra displayed in Fig. 1. The HT voltage increases with a decrease in light transmittance [20]. The two primary causes for reduced transmittance are absorption and light scattering. Light scattering depends on the number and size of aggregates. The HT voltage traces are used here to monitor any significant protein aggregation. The noticeable feature is that the curves associated with AQP0/α-crystallin complex are shifted 2 nm to the red of those with AQP0 alone. It is interesting to note that there is minimal spread in the corresponding HT voltage traces for each of CD spectra measured for AQP0 exposed to different incubation times at 50 °C, suggesting there is insignificant amount of aggregation, and likewise, in the presence of α-crystallin the spread of those HT voltage traces are also insignificant.

4. Discussion

Earlier we have shown that thermal stress, coupled with mechanical agitation, promoted aggregation of detergent-solubilized AQP0, and the presence of α-crystallin prevented that aggregation by its

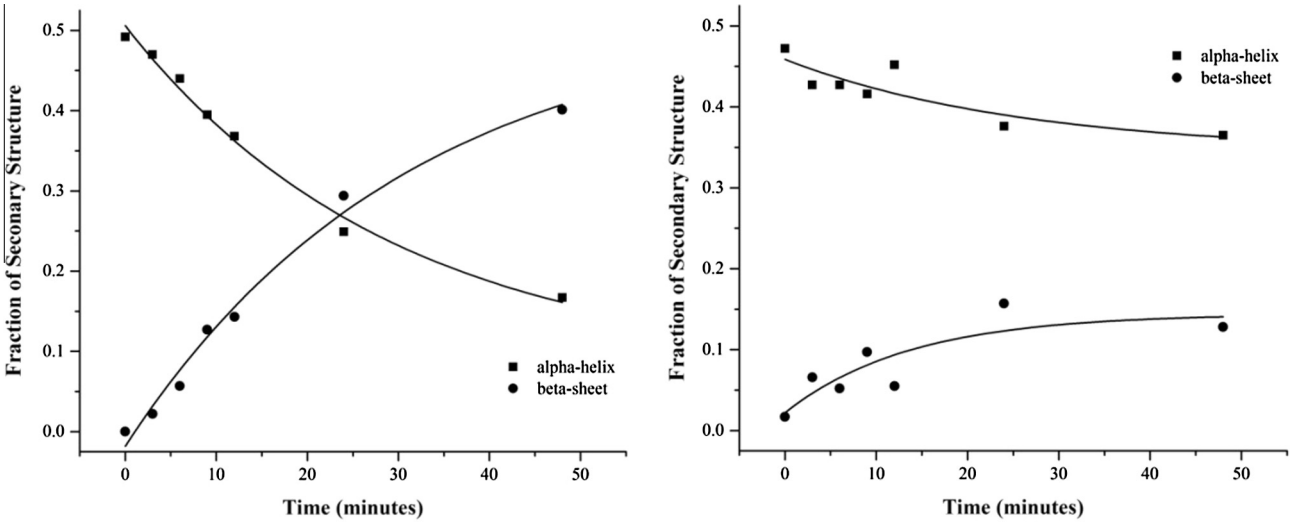

Fig. 3. Time courses showing the fraction of the secondary structural component with the time that AQP0 was subjected to thermal stress. The fraction of each secondary structural component was determined from deconvoluting the spectra shown in Fig. 1. The solid lines are generated from either fitting the loss of α-helical component to an exponential decay or fitting the gain of β-sheet component to an exponential rise. The fitting parameters are listed in Table 1. The *left* and right panels display the change in secondary structural components in the absence and presence of α-crystallin, respectively.

Table 1
Parameters for fitting the time courses of changing secondary structures. These parameters are derived from the Levenberg–Marquardt fitting procedures that produce the curves shown in Fig. 4 and defined by $y(t) = y_0 + A\exp(-t/T)$.

Secondary structure	y_0	A	T (min)
α-Crystallin absent			
α-Helix	0.077 ± 0.048	0.429 ± 0.044	29.5 ± 6.0
β-Sheet	0.523 ± 0.073	−0.541 ± 0.066	31.0 ± 6.5
α-Crystallin present			
α-Helix	0.344 ± 0.065	0.114 ± 0.059	26.2 ± 15.0
β-Sheet	0.144 ± 0.036	−0.136 ± 0.044	21.3 ± 17.0

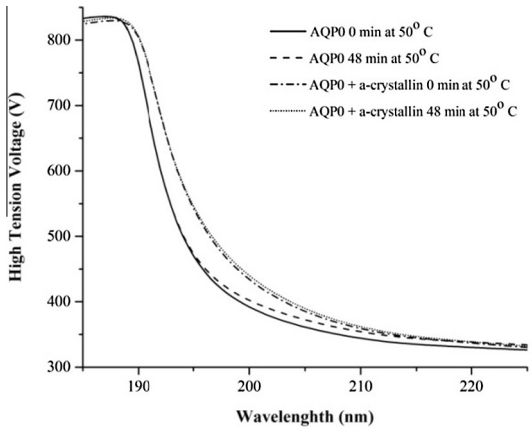

Fig. 4. High Tension voltage traces of AQP0. These are the High Tension (HT) voltage traces associated with the CD spectra of AQP0 before thermal stress (—), following thermal stress at 50 °C for 48 min (– –), before thermal stress with α-crystallin present (– • –) and following thermal stress at 50 °C for 48 min with α-crystallin present (• • •).

chaperone function [16]. The focus of this study is to delineate the effect of thermal stress from the mechanical agitation, and to understand secondary structural changes of AQP0 prior to aggregation.

Similar to native membrane environment, when AQP0 is solubilized in OG, an anionic detergent, it maintains the tetrameric conformation [21,22]. Even in the native membrane environment, AQP0 does undergo heat-induced aggregation above 90 °C, whereas in the micellar environment, the aggregation occurs at much lower temperature (45 °C) [16,23]. Detergent solubilized AQP0 allowed us to carefully follow the secondary structural changes prior to aggregation. Fig. 1 shows time-dependent changes in secondary structures of AQP0 when subjected to thermal stress at 50 °C. The CCA program was an exceptional tool for deconvoluting this set of CD spectra simultaneously. In changing a single experimental parameter – the time that AQP0 is subjected to thermal stress – the common structural features shared by the protein at different degrees of denaturation were extracted. Deconvolution of the CD spectrum into pure components of AQP0, prior to thermal stress, yielded a composition of 51 ± 8% α-helix and 0 ± 12% β-sheet (left panel of Fig. 3 and Table 1), which is in fairly good agreement with the X-ray crystallographic data (60% α-helix and 0% β-sheet) shown by Harris et al. [24]. The amplitude of the common structural features (shown in left panel of Fig. 2) was followed during the course of thermal denaturation of AQP0. The diminution of α-helical structure was used as a measure for the loss of native-like structure. It is apparent from Fig. 3 (left panel) that concomitant with the loss α-helical structure was a gain of β-sheet structure.

Decrease in α-helical structure of AQP0 during thermal denaturation is supported by an exponential decay with a time constant of 29.5 ± 6.0 min (Fig. 3 and Table 1), which corresponds to a first order rate constant of 3.38×10^{-2} min^{-1}. This suggests that the loss of native-like structure is a first order rate process, and not driven by the protein–protein interactions between neighboring micelles. It is also apparent in Fig. 3 that the rate of increase in β-sheet structure is supported by an exponential rise with a time constant of 31.0 ± 6.5 min (see Table 1), which corresponds to a first order rate constant of 3.23×10^{-2} min^{-1}. The close similarity in the two rate constants suggests that the transition from a mostly α-helical structure to a mostly β-sheet structure is highly cooperative. Along with the consideration that the overlay of CD spectra (left panel of Fig. 1) exhibits an isosbestic point is strongly supportive that the denaturation of detergent solubilized AQP0 follows a two state mechanism. Thus, the irreversible conversion from the native-like structure to the denatured protein occurs over a single transition. Previous studies also showed that detergent solubilized glycerol facilitator (a member of aqua-glyceroporin family of proteins) exhibits some cooperative unfolding under thermal

stress [25]. This differs from the pathway arrived at by molecular dynamics simulations for amyloidogenic transitions, which argues that α-helical to β-sheet structures goes through several intermediates [2].

In our earlier studies we have shown that the presence of α-crystallin minimized the aggregation of AQP0 [16], possibly by inhibiting the α-helical to β-sheet transition (see Fig. 3). This gives credence to the view that the formation of β-sheet structure precedes thermal stress induced aggregation of AQP0. α-Crystallin, by its chaperone function, binds to partially unfolded α-helical structures of AQP0 and stabilizes those structures (Fig. 3, right panel). Unlike what we observed in the absence of α-crystallin, in the presence of α-crystallin, loss of α-helical structure does not occur over a single transition, as evidenced by the lack of defined isosbestic point (Fig. 1, right panel). The nature and residues involved in the AQP0 and α-crystallin interaction need to be elucidated.

In our previous work [16], the aggregation of detergent solubilized AQP0 was affected by thermal stress coupled with the shear stress from gentle stirring. It has been pointed out that regular β-sheet edges are in the right conformation to interact with any other β-strand they encounter, which then leads to aggregation [26]. In the present study, in the absence of mechanical sheer, there is no apparent aggregation (Fig. 4). It is reasonable to assume that AQP0 is initially converted to a β-sheet structure and gentle stirring then assists in bringing about the protein–protein contact necessary for aggregation. Unlike proteins containing natural β-sheets, which have inherent edge protection strategies; the α-helices of AQP0 collapse into β-sheet structure, which are prone to aggregation.

Physiological relevance of this study lies in the fact that lens membranes proteins also undergo metabolic and environmental stresses and the presence of α-crystallin in close proximity facilitates stabilizing these proteins, particularly the cytosolic side of the AQP0. Cataracts, which take decades to develop, may be the end result of continued stress coupled with progressive loss of chaperone function of α-crystallin.

Acknowledgments

This research was supported by Grants from the National Science Foundation-United States (DUE-9751530, MRI 0521238, HRD 1305041) and Georgia BOR, STEM II Initiative (UWise). The authors also thank the University of West Georgia for support of this research through Faculty Research and Student Research Assistant Grant programs.

References

[1] H.R. Patel, A.S. Pithadia, J.R. Brender, C.A. Fierke, A. Ramamoorthy, In search of aggregation pathways of IAAPP and other amyloidogenic proteins: finding answers through NMR spectroscopy, J. Phys. Chem. Lett. 5 (2014) 1864–1870.
[2] Q. Ruxi, Y. Luo, B. Ma, R. Nussinov, G. Wei, Conformational distribution and α-helix to β-sheet transition of human amylin fragment dimer, Biomacromolecules 15 (2014) 122–131.
[3] M.A. Speed, D.C. Wang, J. King, Specific aggregation of partially folded polypeptide chains: the molecular basis of inclusion body composition, Nat. Biotechnol. 14 (1996) 1283–1287.
[4] C.M. Dobson, Protein misfolding diseases: getting out of shape, Nature 418 (2002) 729–730.
[5] F. Chiti, N. Taddei, F. Baroni, C. Capanni, M. Stefani, G. Ramponi, C.M. Dobson, Kinetic partitioning of protein folding and aggregation, Nat. Struct. Biol. 9 (2002) 137–143.
[6] F. Ding, J.J. LaRocque, N.V. Dokholyan, Direct observation of protein folding, aggregation, and a prion-like conformational conversion, J. Biol. Chem. 280 (2005) 40235–40240.
[7] J.S. Philo, T. Arakawa, Mechanisms of protein aggregation, Curr. Pharm. Biotechnol. 10 (2009) 348–351.
[8] F.U. Hartl, A. Bracher, M. Hayer-Hartl, Molecular chaperones in protein folding and proteostasis, Nature 475 (2011) 324–332.
[9] R.L.M. van Montfort, E. Basha, K.L. Friedrich, C. Slingsby, E. Vierling, Crystal structure and assembly of a eukaryotic small heat shock protein, Nat. Struct. Biol. 8 (2001) 1025–1030.
[10] K. Niforou, C. Cheimonidou, I.P. Trougakos, Molecular chaperones and proteostasis regulation during redox imbalance, Redox Biol. 2 (2014) 323–332.
[11] A. Engle, H. Stahlberg, Aquaglyceroporins: channel proteins with a conserved core, multiple functions, and variable surfaces, Int. Rev. Cytol. 215 (2002) 75–104.
[12] M.B. Gorin, S.B. Yancey, J. Cline, J.-P. Revel, J. Horwitz, The major intrinsic protein (MIP) of the bovine lens fiber membrane: characterization and structure based on cDNA cloning, Cell 39 (1984) 49–59.
[13] R.T. Mathias, J.L. Rae, The lens: local transport and global transparency, Exp. Eye Res. 78 (2004) 689–698.
[14] E.L. Benedetti, I. Dunia, H. Bloemendal, Development of junctions during differentiation of lens fibers, Proc. Natl. Acad. Sci. 71 (1974) 5073–5077.
[15] S.S. Kumari, K. Varadaraj, Intact AQP0 performs cell-to-cell adhesion, Biochem. Biophys. Res. Commun. 390 (2009) 1034–1039.
[16] S. Swamy-Mruthinti, V. Srinivas, J.E. Hansen, C.M. Rao, Thermal stress induced aggregation of Aquaporin 0 (AQP0) and protection by α-crystallin via its chaperone function, PLoS One 8 (2013) e80404, http://dx.doi.org/10.1371/journal.pone.0080404.
[17] R.E. Perry, M.S. Swamy, E.C. Abraham, Progressive changes in lens crystallin glycation and high-molecular-weight aggregate formation leading to cataract development in streptozotocin-diabetic rats, Exp. Eye Res. 44 (1987) 269–282.
[18] A. Perczel, K. Park, G.D. Fasman, Analysis of the Circular Dichroism spectrum of proteins using the convex constraint algorithm, Anal. Biochem. 203 (1992) 83–93.
[19] K. Park, A. Perczel, G.D. Fasman, Differentiation between transmembrane helices and peripheral helices by the deconvolution of Circular Dichroism spectra of membrane proteins, Protein Sci. 1 (1992) 1032–1049.
[20] S.M. Kelly, T.J. Jess, N.C. Price, How to study proteins by Circular Dichroism?, Biochim Biophys. Acta 1751 (2005) 119–139.
[21] T. Aerts, J.-Z. Xia, H. Slegers, J. de Block, J. Clauwaert, Extraction in n-octyl-β-D-glucopyranoside and evidence for a tetrameric structure, J. Biol. Chem. 265 (1990) 8675–8680.
[22] A. Berthaud, J. Manzi, J. Perez, S. Mangenot, Modeling detergent organization around Aquaporin-0 using small angle X-ray scattering, J. Am. Chem. Soc. 134 (2012) 10080–10088.
[23] R.M. Broekhuyse, E.D. Kuhlmann, Lens membranes V. The influence of reduction and heating on the electrophoretical polypeptide pattern of lens fiber membranes, Exp. Eye Res. 28 (1979) 615–618.
[24] W.E.C. Harries, D. Akhavan, L.J.W. Miercke, S. Khademi, R.M. Stroud, The chemical architecture of Aquaporin 0 at a 2.2-A resolution, Proc. Natl. Acad. Sci. U.S.A. 101 (2004) 14045–14050.
[25] J.J. Galka, S.J. Baturin, D.M. Manley, A.J. Kehlar, J.D. ONeil, Stability of glycerol facilitator in detergent solutions, Biochemistry 47 (2008) 3513–3524.
[26] J.S. Richardson, D.C. Richardson, Natural β-sheet proteins use negative design to avoid edge-to-edge aggregation, Proc. Natl. Acad. Sci. U.S.A. 99 (2002) 2754–2759.